Repeat Motions and Backbone Flexibility in Designed Proteins with Different Numbers of Identical Consensus Tetratricopeptide Repeats†

Cecilia Y. Cheng,‡,⊥ Virginia A. Jarymowycz,‡,⊥ Aitziber L. Cortajarena,§ Lynne Regan,§,|| and Martin J. Stone*,‡

Department of Chemistry, Indiana University, Bloomington, Indiana 47405-0001, and Department of Molecular Biophysics and Biochemistry and Department of Chemistry, Yale University, P.O. Box 208114, 266 Whitney Avenue, New Haven, Connecticut 06520-8114

Received April 26, 2006; Revised Manuscript Received July 28, 2006

ABSTRACT: The tetratricopeptide repeat (TPR) is a 34-residue helix-turn-helix motif that occurs as three or more tandem repeats in a wide variety of proteins. We have determined the repeat motions and backbone fluctuations of proteins containing two or three consensus TPR repeats (CTPR2 and CPTR3, respectively) using ^{15}N NMR relaxation measurements. Rotational diffusion tensors calculated from these data for each repeat within each TPR protein indicate that there is a high degree of motional correlation between different repeats in the same protein. This is consistent with the prevailing view that repeat proteins, such as CTPR2 and CTPR3, behave as single cooperatively folded domains. The internal motions of backbone NH groups were determined using the Lipari−Szabo model-free formalism. For most residues, there was a clear separation between the influence of internal motion and the influence of global rotational tumbling on the observed magnetic relaxation. The local internal motions are highly restricted in most of the helical elements, with slightly greater flexibility in the linker elements. Comparisons between CTPR2 and CTPR3 indicate that an addition of a TPR repeat to the *C*-terminus (before the solvation helix) of CTPR2 slightly reduces the flexibility of the preceding helix.

A large number of proteins contain domains composed of tandem repeats of structurally similar motifs (*1*, *2*). These repeat proteins differ from globular proteins composed of tandem domains in that the interactions between consecutive repeating units are highly regular and relatively short-range. The prevalence of repeat proteins may be related to their ability to evolve readily, through cycles of gene duplication and subsequent mutation, allowing them to acquire new specificities or possibly novel biochemical functions. In addition, their extended non-globular structures may present a large surface area for interaction with other molecules.

To assess the influences of adjacent repeats on each other, it is necessary to understand not only their structures but also the degree to which each repeat can move independently of its neighbors, that is, the flexibility or dynamics of the protein. X-ray crystal structures of both tetratricopeptide repeat (TPR[1]) proteins and ankyrin repeat proteins indicate that the individual modules of repeat proteins are tightly associated in the folded state (*3*, *4*), consistent with spectroscopic measurements and theoretical modeling of highly cooperative folding thermodynamics (*3*, *5*−*10*). In the case of ankyrin repeat proteins, there is also direct evidence from NMR relaxation data that the individual repeats tumble as a single unit rather than independent domains (*11*). However, hydrogen exchange data have demonstrated hierarchical unfolding with faster exchange in the terminal repeats than in the central repeats (*5*, *12*).

Here, we describe a study of the effect of the number of identical, tandem TPR repeats on a protein's internal flexibility and dynamics. TPR domains (consisting of several tandem repeats) are thought to mediate protein−protein interactions and play an essential role in a variety of cellular processes from chromatin remodeling to protein import into mitochondria and protein folding (*2*, *13*). Main et al. (*3*) have recently reported the design of three proteins consisting of 1−3 consensus TPR repeats (CTPR1, CTPR2, and CPTR3, for consensus TPR number of repeats). The consensus TPR sequence, on which these designs are based, was obtained from a statistical analysis of the sequences of all individual TPR motifs. CTPR1, 2, and 3 form well-defined folded structures in solution, as defined by CD and NMR, and the X-ray crystal structures of CTPR2 and CTPR3 confirm that each of the repeats adopts the typical TPR fold. The stability of the protein increases with the number of tandem repeats; the T_m values of CTPR1, CTPR2, and CTPR3 are 49, 74, and 83 °C, respectively (*3*). Amide solvent hydrogen exchange measurements on CTPR2 and CTPR3 suggested

† This work was supported by a grant awarded to M.J.S. from the National Science Foundation (MCB-0212746).

* Corresponding author: Phone: (812) 855-6779. Fax: (812) 855-8300. E-mail: mastone@indiana.edu.

‡ Indiana University.

§ Department of Molecular Biophysics and Biochemistry, Yale University.

|| Department of Chemistry, Yale University.

⊥ These authors contributed equally to this work.

[1] Abbreviations: CD, circular dichroism; η_{xy}, transverse cross-relaxation rate constant; HSQC, heteronuclear single quantum coherence spectrum; NMR, nuclear magnetic resonance; NOE, nuclear Overhauser effect; R_1, longitudinal relaxation rate constant; R_2, transverse relaxation rate constant; R_{ex}, exchange contribution to transverse relaxation; S^2, order parameter; τ_e, effective internal correlation time; τ_m, molecular rotational correlation time; TPR, tetratricopeptide repeat.

10.1021/bi060819a CCC: $33.50
Published on Web 09/09/2006

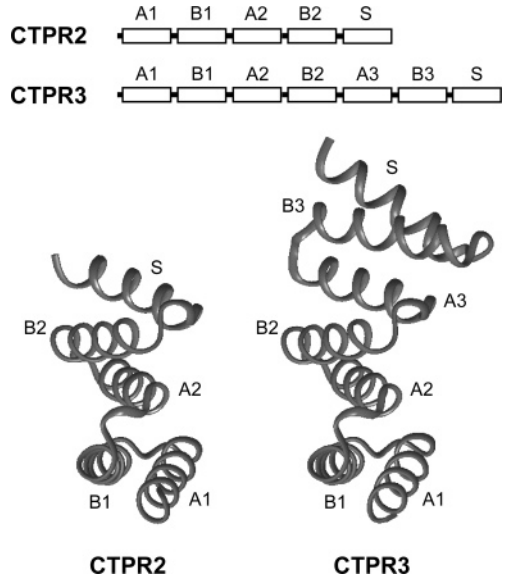

FIGURE 1: Structures and repeat organization of CTPR2 and CTPR3. Top: schematic diagrams indicating the positions and nomenclature for each of the helices (open bars) in each protein; A and B indicate the first and second helix of each repeat, respectively, whereas S indicates the *C*-terminal solvation helix. Bottom: ribbon diagrams showing the X-ray structures of the two proteins with each helix labeled.

that the central region of each protein exchanges through a global unfolding mechanism, whereas the outer regions exchange through sub-global unfolding (*5*). More recently, the unfolding transitions for proteins containing 2−10 consensus TPR repeats, all of which show a single cooperative unfolding transition, have been described quantitatively by a simple Ising model, which includes an identical unfolding free energy for every helix and a single coupling parameter for pairs of adjacent helices (*6*).

Figure 1 shows a schematic representation of the secondary structures of CTPR2 and CTPR3, the nomenclature used in this article to refer to each helical element, and a ribbon representation of the X-ray crystal structures of the proteins. As in natural TPR proteins (*14*), each repeat consists of a pair of 13−14 residue α-helices (A and B) packed together at an angle of ∼160°. Each repeat is stacked against adjacent repeats, with extensive contacts formed between the B helix of one repeat and the A helix of the following repeat. The packing gives rise to a superhelical arrangement of repeats with a predicted periodicity of ∼8 repeats per superhelical turn (Kajander, T., Cortajarena, A. L., and Regan, L., to be submitted for publication and ref 6 (*6*)).

An important property of the CTPR proteins is that the individual TPR repeats within them are all identical. Thus, comparing the properties of the repeats in these proteins should reveal differences due to the lengths and stabilities of the proteins or the structure and dynamics of adjacent repeats, rather than the internal composition of each repeat. Consequently, the CTPR proteins provide an excellent system in which to investigate the factors (other than local sequence variation) that influence both repeat reorientation and internal flexibility in repeat proteins.

Reorientation of small domains in proteins occurs on timescales of several nanoseconds and can be readily detected by measuring the magnetic relaxation properties of nuclei within each domain (*15*−*17*). An advantage of this approach is that, in favorable cases, relaxation data can be obtained for many nuclei within each domain, allowing one to characterize both the anisotropy of the domain motions and also the subnanosecond internal rotational motions of the bond vectors. Here, we describe the use of ^{15}N NMR relaxation data to characterize both the repeat motions and the local backbone motions of CTPR2 and CTPR3.

MATERIALS AND METHODS

Protein Samples. Uniformly ^{15}N-labeled CTPR2 and CTPR3 were expressed and purified as described previously (*5*), and identity was confirmed by mass spectrometry.

NMR Measurements. NMR samples consisted of 1.0 mM ^{15}N-labeled CTPR2 or CTPR3 in 50 mM sodium phosphate, 150 mM NaCl, 90% H_2O, 10% D_2O at pH 6.3. All NMR experiments were performed at 20 °C on a Varian Unity-INOVA 500 MHz spectrometer with a triple-resonance 3-axis gradient probe. Previously published 2D ^{1}H-^{15}N HSQC style pulse sequences (*18*, *19*) were used to measure the ^{15}N longitudinal (R_1) and transverse (R_2) auto-relaxation rate constants, heteronuclear {^{1}H}-^{15}N NOEs, and ^{15}N transverse cross-relaxation rate constants (η_{xy}). For all experiments, the ^{1}H carrier was set on the water resonance, the ^{15}N carrier was set at 119 ppm, and the spectral widths were 7000 and 1500 Hz for ^{1}H and ^{15}N, respectively. Other experimental parameters were the same as those used in a previous study (*20*) except that the NOE experiments were performed in duplicate rather than quadruplicate. In particular, all relaxation experiments were all performed using 16 transients per FID and 128 complex t_1 increments. Relaxation time delays were 11*, 55, 133, 233*, 377, 555*, 888, and 1998* ms for the R_1 experiment, 17*, 33, 67*, 101, 151, 201*, 285, and 386* ms for the R_2 experiment and 22*, 43, 65*, 76, 98, and 109* ms for the η_{xy} experiment; asterisks indicate time delays that were performed in duplicate in order to assess peak height uncertainties. ^1H_N and $^{15}N_H$ resonance assignments were made using published chemical shift values (*5*); assigned HSQC spectra are given in the Supporting Information. In order to resolve a few ambiguities resulting from minor chemical shift changes relative to the previous study, we also performed 3D TOCSY-HSQC and NOESY-HSQC experiments, with mixing times of 80 and 120 ms, respectively. For these experiments, the ^{1}H and ^{15}N carrier frequencies were the same as those given above, and the spectral widths were 7000, 6000, and 1500 for the indirect ^{1}H, direct ^1H_N, and ^{15}N dimensions, respectively.

Data Analyses. NMR data were processed using Felix98 (Molecular Simulations, Inc., Burlington, Massachusetts), and the relaxation parameters and standard errors were extracted as described (*20*). All overlapped resonances and peaks that were too weak for reliable intensity measurements were omitted from the data analysis. Residues that exhibited large amplitude, fast internal motions (NOE < 0.5), or were influenced significantly by slow time scale conformational exchange (R_2/η_{xy} values that exceeded the average by more than one standard deviation or elevated R_2/R_1 ratios) were identified and removed for the initial estimation of the molecular diffusion tensor. Residues excluded for CTPR2 were Gly-91 (extensive fast internal motion), Asn-14, Ala-28, Asp-39, Gly-50, Tyr-59, Ala-77, Asn-82, Lys-89 (conformational exchange), Ala-9, and Leu-15, whereas residues

excluded for CTPR3 were Gly-125 (extensive fast internal motion), Ile-29, Tyr-59, Tyr-93, Tyr-100, Ala-111, Gln-115, Leu-117, and Asn-119 (conformational exchange). Isotropic, axially symmetric (both prolate and oblate), and fully anisotropic diffusion tensors were each calculated using the program quadric_diffusion (A.G. Palmer, III, Columbia University, NY) from the R_2/R_1 ratios of the remaining residues (53 residues for CTPR2 and 49 residues for CTPR3) and the coordinates of the X-ray structures (pdb files 1NA3 and 1NA0 for CTPR2 and CTPR3, respectively) (*3*). The most appropriate diffusion tensor was selected by comparison of χ^2 and F statistics (see Results and Discussion). Errors in diffusion parameters reported by quadric_diffusion were confirmed by Monte Carlo simulations. Relaxation parameters were fit, using the program Modelfree version 4.0 (A.G. Palmer, III, Columbia University, NY) to five versions of the Lipari−Szabo model-free dynamics formalism (*21*−*24*), in which the fitted parameters are model 1, order parameter (S^2); model 2, S^2 and internal correlation time (τ_e); model 3, S^2 and exchange broadening contribution to transverse relaxation (R_{ex}); model 4, S^2, τ_e, and R_{ex}; and model 5, order parameters for two time scales (S_f^2 and S_s^2) and τ_e for the slower time scale. Initial model-free calculations were executed using the prolate axially symmetric diffusion tensor estimated using quadric_diffusion. After selection of the best internal dynamics model for each residue, as described (*25*), all internal dynamics parameters and the rotational diffusion tensor were optimized simultaneously in a final model-free calculation. Standard errors were obtained from 500 Monte Carlo simulations. The parameter κ, used to assess the degree of correlated motion between repeats, is defined (*15*) as

$$k_{\alpha,\beta} = \mathrm{Tr}(\mathbf{D}_\alpha)/\mathrm{Tr}(\mathbf{D}_\beta)$$

in which α and β refer to the two domains, $\mathbf{D}_\alpha$ and $\mathbf{D}_\beta$ are the diffusion tensors determined independently for the domains, and Tr represents the trace of the tensor, calculated as the sum of the diagonal elements ($D_{xx} + D_{yy} + D_{zz}$).

RESULTS AND DISCUSSION

Relaxation Parameters. Relaxation data were collected for 64 of 87 backbone NH groups for CTPR2 and 58 of 120 backbone NH groups for CTPR3; the derived parameters are listed in the Supporting Information. The sequence coverage, which is lower (74% and 48%, respectively) than that for typical globular proteins, can be attributed primarily to the high level of resonance overlap, which is a consequence of the tandem repeats having identical amino acid sequences. In addition, the amide resonances of the ten amino-terminal residues in each protein are not observable. Nevertheless, the relaxation data obtained for each protein are derived from backbone NH groups well spread throughout the TPR repeats with 26 and 24 residues in repeats 1 and 2, respectively, of CTPR2 and 18, 15, and 13 residues in repeats 1, 2, and 3, respectively, of CTPR3.

The R_1, R_2, and NOE values and the R_2/R_1 ratios for each residue in each protein are plotted in Figure 2A−D. Residues in CTPR2 exhibit faster longitudinal relaxation (R_1) and slower transverse relaxation (R_2) than equivalent residues in CTPR3, consistent with the differences in molecular masses (CTPR2 = 10.3 kDa, CTPR3 = 14.4 kDa). However, NOE values are very similar for both proteins, suggesting that their internal motions are comparable. For both proteins, the relaxation parameters are fairly uniform across the sequence.

Several residues stand out as having unusual properties. First, the *C*-terminal residues of both proteins (Gly-91 of CTPR2 and Gly-125 of CTPR3) have dramatically lower than average values of R_2, NOE, and R_2/R_1, which is indicative of extensive fast internal motions. Second, residues Ala-28, Asn-41, and Ala-77 of CTPR2 and residues Ala-28, Asn-41, and Asn-75 of CTPR3 have R_2 values elevated above those for other residues. High R_2 values can arise from an alignment of the NH vector with the long axis of the molecule, which causes relatively slow reorientation of the bond vector. Alternatively, the high R_2 values could result from conformational exchange on a time scale of microseconds to milliseconds. We were able to distinguish between these possibilities by comparing the R_2 values with the transverse cross relaxation rates (η_{xy}; Figure 2E and F) (*19*) and by observation of conformational exchange broadening contributions in the extended model-free analysis (*vide infra*).

Evidence for conformational exchange was found for two distinct regions. First, both Ala-77 of CTPR2 and the equivalent residue (Ala-111) of CTPR3 exhibited high values of R_2/η_{xy}, suggesting a possible structural fluctuation near the amino terminus of the solvation helix in both proteins. Second, residue Ala-28 in CTPR2 exhibited evidence of slow conformational exchange broadening but this was not observed for the equivalent residue in CTPR3 or for corresponding residues in other repeats of either protein. This raises the possibility of a relatively slow (microsecond-millisecond time scale) conformational rearrangement occurring in the first repeat of CTPR2 but not in CTPR3 or in other repeats of either protein. One possibility is that this involves a local unfolding rearrangement, consistent with the relatively high rate of hydrogen exchange previously observed in this repeat (*5*).

The analysis of R_2/η_{xy} values also indicated that the elevated transverse relaxation rates observed for residues Asn-41 of both proteins and Asn-75 of CTPR3 could not be attributed to conformational exchange, thus suggesting that the backbone NH groups of these residues may be aligned with the long axis of the molecule. Indeed, the subsequent diffusion tensor optimization indicated that these residues (located in the turns following helices B1 or B2) are the only observed NH groups whose angles to the long axis are less than 30° (angles of 6° for Asn-41 of CTPR2 and 12° for both Asn-41 and Asn-75 of CTPR3). Notably, Asn-41 and Asn-75 of CTPR3 are exactly one repeat (34 residues) apart; therefore, these results suggest that the long axis of the molecule may be almost parallel with the superhelical axis for CTPR3, which is consistent with the overall shape of the molecule (Figure 1).

Rotational Diffusion and Repeat Motions. To investigate whether the repeat units of the CTPR proteins undergo segmental motions relative to each other, we characterized the rotational diffusion of each TPR repeat separately and compared it to the rotational diffusion calculated for each molecule as a whole. In each calculation, the diffusion tensor was calculated from the R_2/R_1 ratios of NH groups that do not exhibit evidence of either large amplitude fast internal motions (low NOE) or slow conformational exchange (high R_2/η_{xy}); relative orientations of the bond vectors were obtained from the X-ray structures (*3*).

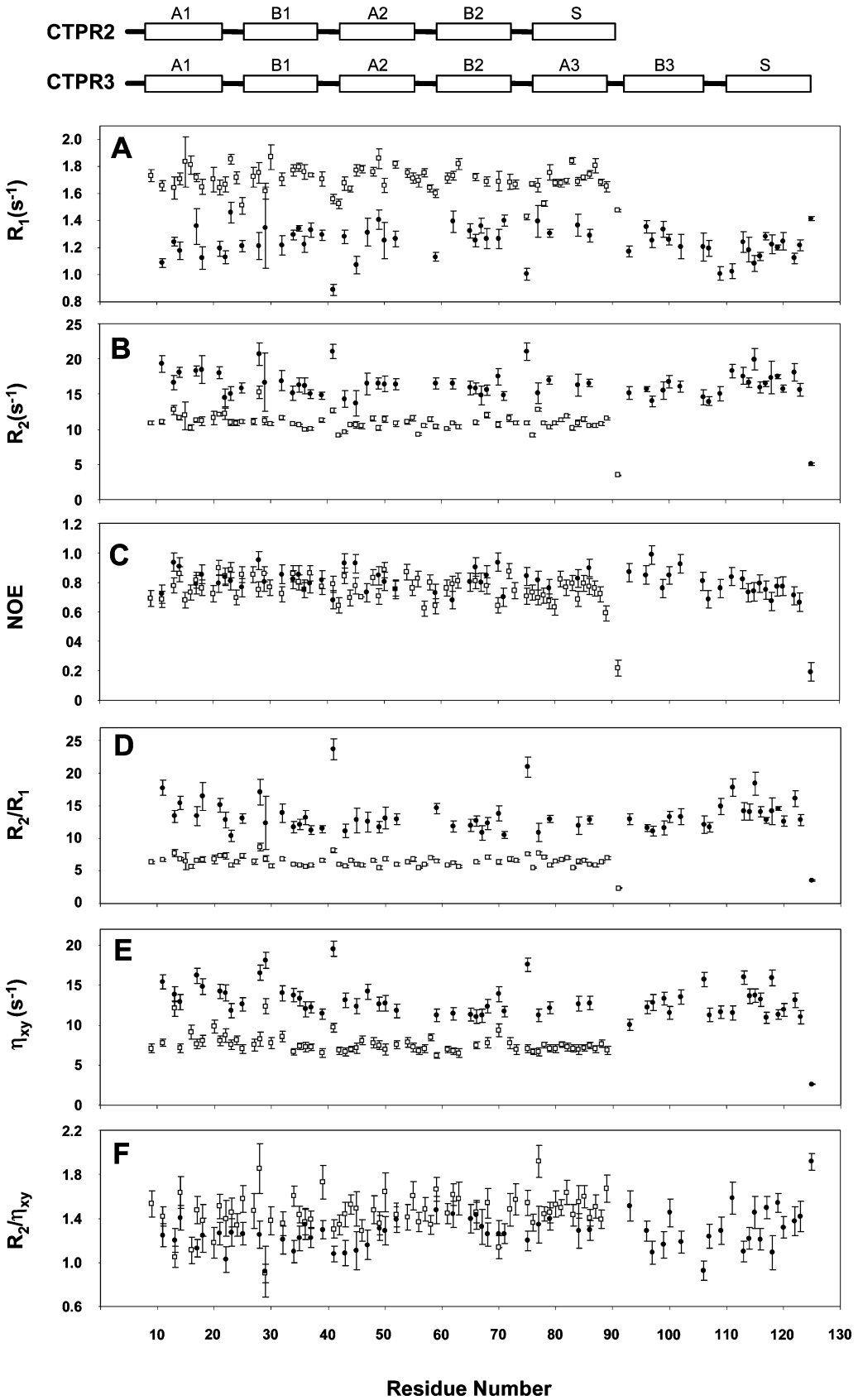

FIGURE 2: Relaxation data for CTPR2 (□) and CTPR3 (●) as a function of residue number: (A) R_1; (B) R_2; (C) NOE; (D) R_2/R_1; (E) η_{xy}; and (F) R_2/η_{xy}. The positions of the helical elements (open bars) are indicated schematically at the top.

For each intact protein and for most individual repeats, a prolate axially symmetric diffusion tensor fit the data substantially better than an oblate axially symmetric model. For repeats 1 and 3 of CTPR3, the oblate model was slightly preferred, but the χ^2 parameters for the two models differed by <10%. For consistency, we selected the prolate model for subsequent calculations and comparisons. In every case, the prolate axially symmetric diffusion tensor afforded a

Table 1: Diffusion Parameters for Each Protein and Each Individual Repeat[a]

protein	region (residue nos.)	no. of residues	τ_m (ns)	$D_\parallel/D_\perp$	θ (deg)	ϕ (deg)
CTPR2	all (1−83)	53	9.06 ± 0.16	1.46 ± 0.08	83 ± 4	162 ± 7
CTPR2	repeat 1 (11−42)	21	8.97 ± 0.08	1.47 ± 0.07	94 ± 5	175 ± 4
CTPR2	repeat 2 (43−76)	22	9.65 ± 0.67	2.01 ± 0.57	84 ± 7	145 ± 17
CTPR3	all (1−125)	49	13.93 ± 0.40	1.86 ± 0.17	94 ± 7	131 ± 6
CTPR3	repeat 1 (11−42)	17	14.17 ± 0.53	2.17 ± 0.49	84 ± 16	133 ± 7
CTPR3	repeat 2 (43−76)	14	13.98 ± 1.02	2.10 ± 0.71	67 ± 11	120 ± 17
CTPR3	repeat 3 (77−110)	11	14.25 ± 0.49	2.07 ± 0.50	90 ± 4	27 ± 11

[a] Parameters are reported for the axially symmetric diffusion model. $D_\parallel$ and $D_\perp$ are the diffusion constants around the unique and perpendicular axes, respectively: $\tau_m = (2D_\parallel + 4D_\perp)^{-1}$; and ϕ and θ are the Euler angles defining the axis system of the diffusion tensor relative to the inertial tensor, as reported by the program quadric_diffusion.

statistically significant improvement over an isotropic diffusion tensor ($F > F_{0.95}$), whereas a fully anisotropic diffusion tensor did not significantly improve the fit relative to that of the prolate axial model ($F < F_{0.95}$).

The diffusion tensors determined for each protein and each individual repeat are compared in Table 1. The rotational correlation times (τ_m) for intact CTPR2 and each individual repeat of CTPR2 are ~9 ns, whereas those for intact CTPR3 and each individual repeat of CTPR3 are ~14 ns. This difference corresponds closely to the difference in the molecular masses of the two intact proteins. Moreover, the similar τ_m values obtained for the individual repeats in comparison to the protein as a whole suggest that the rotational motions of the repeats within one protein are highly correlated. This is particularly evident for CTPR3, in which the effective correlation times of the outer repeats differ from that of the central repeat by <3%. Although the diffusion parameters for individual repeats are generally very similar to those for the whole protein, the ϕ angle for the third repeat of CTPR3 differs noticeably from the ϕ angles for the first two repeats. Considering the similarity of τ_m values for all three repeats, we believe that this difference is most likely a consequence of the inadequate sampling of orientational space because of the limited number of probes in the third repeat (four in helix A3 and seven in helix B3, rather than an indication of a real difference in motion.

Brüschweiler and colleagues (*15*) have introduced the parameter κ as a means by which to quantify the degree of correlated motion between two domains of a multidomain protein. If two domains have no independent motion, then $\kappa = 1$. Thus, pairs of strongly correlated domains, with very similar diffusion tensors, yield κ values close to one. A caveat of this treatment is that pairs of domains that have independent motion can also give a value of $\kappa = 1$ if the sum of the diffusion components ($D_{xx} + D_{yy} + D_{zz}$) is, by coincidence, the same for the two domains. However, κ values substantially greater than one can only be explained by the presence of segmental motions.

The κ values calculated from the axially symmetric diffusion tensors for CTPR3 are $\kappa_{2,1} = 1.02 \pm 0.26$ (reporting on correlated motion between repeat 1 and repeat 2) and $\kappa_{3,2} = 1.02 \pm 0.26$ (reporting on correlated motion between repeat 2 and repeat 3), and the corresponding value for the two repeats of CTPR2 is $\kappa_{1,2} = 1.13 \pm 0.17$. Considering that these values are not significantly different from unity or from each other, our data do not provide any evidence for segmental repeat motions in these proteins. This conclusion is consistent with the previous observation that the five ankyrin repeats of cyclin-dependent kinase inhibitor $p19^{INK4d}$ showed no systematic variations of relaxation (or spectral density) parameters between repeats, suggesting that $p19^{INK4d}$ behaves as a fairly rigidly packed protein (*11*). In contrast, proteins consisting of strings of independent domains (as opposed to repeat proteins, where there are extensive inter-repeat interactions) can display various levels of segmental motions between domains. Examples include high correlation between tandem SH3 and SH2 domains of the Abelson kinase (*11*, *15*, *16*, *26*−*30*); significant segmental motions between the two EF hands in free calmodulin (*16*, *29*), with the motion being frozen upon peptide binding (*29*, *30*); and tighter coupling between the first two repeats than that between the second and third repeats of zinc finger transcription factor TFIIIA (*15*).

Internal Dynamics. The internal dynamics of the backbone NH groups in CTPR2 and CTPR3 were determined using the Lipari−Szabo model-free formalism (*21*, *22*). The formalism is referred to as model-free because it does not assume any particular physical description for the motion. However, the possible mathematical representations of the formalism (models 1−5, Materials and Methods) were designed to describe several specific situations. In particular, models 1 and 2 will only satisfy the data adequately if the internal rotational motions occur on a time scale substantially faster than the overall rotational diffusion, whereas models 3−5 describe more complex situations (see Materials and Methods). The common parameter reported by all models is the order parameter (S^2) for each NH bond vector, representing the degree of motional restriction of that bond vector on a time scale faster than a few hundred picoseconds, that is, more than 20-fold faster than the overall tumbling in the case of CTPR2 and CTPR3. The value of S^2 ranges from 0 (completely unrestricted motion) to 1 (completely restricted motion).

Initial model-free calculations were performed under the assumption that each protein undergoes axially symmetric rigid-body rotational diffusion, as determined above, rather than segmental motions of the different repeats. In addition, we performed model-free optimizations for each repeat of each protein using the axially symmetric rotational diffusion tensor determined independently for that repeat. Internal dynamics parameters determined using the latter method did not differ significantly from those obtained by using rigid-body rotation of the whole molecule (data not shown). Therefore, below we discuss only the dynamics parameters from the rigid-body calculations.

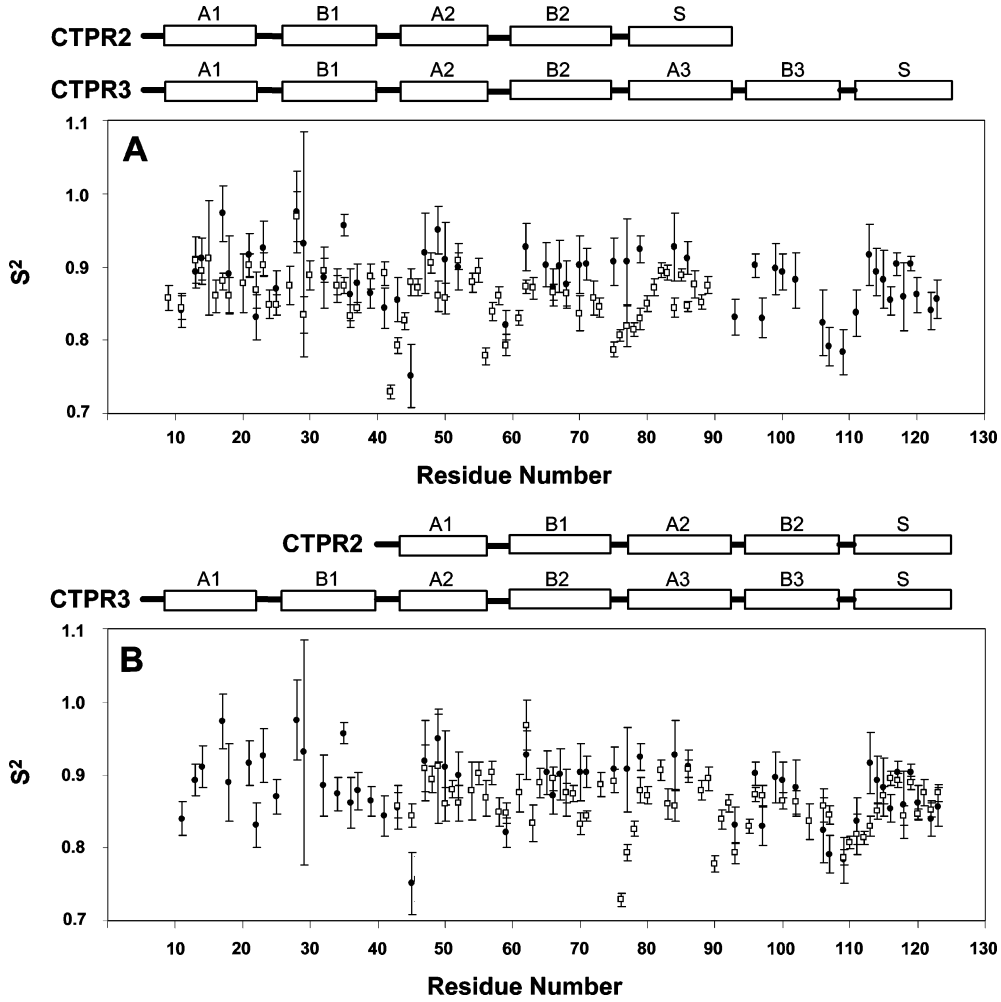

FIGURE 3: Order parameters for CTPR2 (□) and CTPR3 (●) aligned beginning at the amino-terminus (A); and beginning at the carboxy-terminus (B), as indicated by the schematic diagrams above each panel. The residue numbers indicated for panel (B) correspond to those for CTPR3. Order parameters are not shown for residues that were fit to two time scales of internal motion (model 5).

The relaxation data for most bond vectors (62 of 64 in CTPR2 and 57 of 58 in CTPR3) could be accounted for using either model 1 (S^2 only) or model 2 (S^2 and τ_e). Among the remaining few NH vectors, Ala-77 of CTPR2 required the addition of a parameter (R_{ex}) to account for the microsecond-millisecond time scale conformational exchange (*vide supra*), whereas the data for the *C*-terminal residues of both proteins (Gly-91 and Gly-125) could only be fit adequately by incorporating a second time scale of internal motion on the order of ~1.5−2 ns. In summary, for most residues in CTPR2 and CTPR3, there appears to be a clear separation between the influence of internal motion and the influence of global rotational tumbling on the observed magnetic relaxation.

The order parameters calculated for each NH group in CTPR2 and CTPR3 are compared in Figure 3, and the average and standard deviation for each structural element is listed in Table 2. The average (± standard deviation) of order parameters (omitting those fit using model 5) are 0.860 ± 0.038 for CTPR2 and 0.883 ± 0.044 for CTPR3, indicating that these proteins have similar rigidity to typical globular proteins, with relatively small variations throughout each protein. All α-helices have average order parameters in the range 0.85−0.92 (Table 2), whereas several (but not all) of the linkers between the helices display slightly higher mobility with order parameters dropping to 0.7−0.8 in a few cases.

Table 2: Average (± Standard Deviation) of Order Parameters in Each Structural Element

	CTPR2		CTPR3	
element	no. of residues	S^2 average ± SD	no. of residues	S^2 average ± SD
helix A1 (9−21)	10	0.880 ± 0.024	6	0.904 ± 0.043
linker (22−24)	3	0.873 ± 0.027	2	0.879 ± 0.067
helix B1 (25−38)	10	0.874 ± 0.040	8	0.904 ± 0.044
linker (39−42)	3	0.836 ± 0.092	2	0.854 ± 0.014
helix A2 (43−55)	10	0.868 ± 0.036	6	0.881 ± 0.071
linker (56−58)	3	0.826 ± 0.043	0	
helix B2 (59−72)	8	0.849 ± 0.027	8	0.888 ± 0.032
linker (73−76)	3	0.813 ± 0.029	1	0.907 ± 0
helix A3 (77−89)			4	0.918 ± 0.010
linker (90−92)			0	
helix B3 (93−106)			7	0.866 ± 0.035
linker (107−110)			2	0.787 ± 0.006
solvation helix[a]	13	0.858 ± 0.027	11	0.873 ± 0.028

[a] Residues 77−91 in CTPR2 and 111−125 in CTPR3.

When the two protein sequences are aligned beginning at the amino terminus (Figure 3A), it is evident that helix B2 is substantially more flexible in CTPR2 than in CTPR3 ($p = 0.044$, paired *t*-test), whereas other helices (A1, B1, and A2) have similar flexibility in both proteins ($p = 0.22$, 0.11,

and 0.74, respectively); the difference between B1 helices in the two proteins is dominated by a single residue (Ala-35). Not surprisingly, the solvation helix of CTPR2 is also substantially more mobile than the corresponding region (helix A3) in CTPR3 (Figure 3A). Thus, extension of CTPR2 by inserting an additional repeat between repeat 2 and the solvation helix causes rigidification of helix B2 but does not affect the flexibility of helix A2 or the flexibility of repeat 1. It is possible that this rigidification results from tighter packing of helix B2 to helix A3 in CTPR3 in comparison with the packing of helix B2 to the solvation helix in CTPR2; this occurs despite the fact that the packing residues on both helices are identical (only the outer surface of the solvation helix has been modified) (*3*), although the surface area for the helix B to the solvation helix packing interface is slightly smaller (507 Å) compared to the surface area for the B helix−A helix interface (555 Å), as calculated using the program HIT (*31*). The solvation helix has similar intrinsic helical propensity to the A helix, as assessed using the program AGADIR (*32*). The X-ray structures (*3*) indicate that $C_\alpha - C_\alpha$ distances from helix B2 to the following helix are shorter by an average of 0.28 Å in CTPR3 than that in CTPR2. It is unclear whether this difference alone is sufficient to cause the observed change in flexibility in helix B2. However, the structural difference might be increased in solution. In addition, the higher flexibility of the solvation helix in CTPR2, compared to that in helix A3 in CTPR3, could also allow increased motion of the B2 helix in the shorter protein.

The interpretation that differences in dynamics of helix B2 are caused by differing interactions with the following helix is confirmed by the alternative comparison of the data shown in Figure 3B, in which the two protein sequences are aligned beginning at the *C*-terminus (by shifting the CTPR2 sequence by 34 residues). It now becomes clear that helix B3 of CTPR3 has similar flexibility to helix B2 of CTPR2 ($p = 0.67$) and that the solvation helices of both proteins also have similar flexibility ($p = 0.22$). Other corresponding pairs of helices (A1/A2, B1/B2) also have similar flexibility in both proteins ($p = 0.76$ and 0.97, respectively); a slight difference ($p = 0.085$) between helices A2 (CTPR2) and A3 (CTPR3) is based upon only 4 residues, mostly located near the ends of the helices and may not be representative of the internal flexibility of these helices. In summary, the data indicate that extending the amino terminus of CTPR2 by one repeat does not substantially influence the internal flexibility of the remainder of the protein. Thus, our data suggest that internal motions of a TPR repeat (on the picosecond the nanosecond time scale) may be influenced to a greater extent by interactions with the following repeat than those with the preceding repeat.

The order parameters discussed above were calculated under the assumption that each protein rotates as a rigid body. Therefore, the presence of segmental motions of the repeats could cause artifacts in the calculated internal dynamics parameters. To ensure that the lower order parameters discussed above for CTPR2 did not result from such an artifact, we performed a series of model-free calculations for CTPR2 in which the molecular correlation time (τ_m) was varied over the range 7.0−10.2. The reduction of τ_m from 9.0 to 8.0 ns caused an average reduction (rather than increase) in the calculated S^2 values of 0.022. Thus, the low order parameters observed for CTPR2 are not an artifact of segmental motions.

Dynamics as a Criterion for Protein Design. Despite important progress in the rational design of protein structures, it remains challenging to design proteins whose physical properties are similar to those of naturally occurring globular proteins. One criterion for native-like structure would be for the designed protein to display internal dynamics similar to those of natural proteins because this may be reflective of well-defined packing as opposed to a disordered core (molten-globule). In a previous study of a *de novo* designed three-helix bundle protein, Walsh et al. found that the backbone dynamics are highly restricted ($S^2 \sim 0.8$ for NH groups) but that the methyl-bearing side chains are more flexible than that typically observed in natural proteins (*33*). Thus, one could view restricted backbone dynamics as being necessary but not sufficient to define native-like tertiary structure. Although data for side chain mobility are not yet available, the observations that CTPR2 and CTPR3 have high backbone order parameters and that the repeats of each protein tumble with very similar correlation times are consistent with the proposal that these proteins are native-like in solution as well as in the crystal state (*3*). Notably, comparisons of the structures of the designed CTPR3 and the longer designed CTPR8 and CTPR20 with the structures of comparable natural TPR domains (Kajander, T., Cortajarena, A. L., and Regan, L., to be submitted for publication and refs 14 and 34−38 (*14*, *34*−*38*)), reveals a conservation of inter-repeat interactions and, hence, superhelical parameters in all of the proteins.

Comparison to Hydrogen Exchange Studies of Repeat Proteins. A number of previous studies have investigated the conformational fluctuations of repeat proteins using H−D exchange experiments (*5*, *12*). Of particular relevance here, the CTPR2 and CTPR3 proteins exhibit facile hydrogen exchange in their terminal helices (A1 and the solvation helix) and progressively increasing protection moving toward the center of each protein (*5*). A similar pattern was observed for a protein phosphatase 5 fragment containing 3.5 TPR repeats (*39*) and for the transcriptional regulator IκBα, which consists of six ankyrin repeats (*12*). The H−D exchange data for the CTPR proteins contrasts sharply with the picosecond time scale dynamics, which show a similar degree of restriction in all helices (Table 2, Figure 3), although very fast hydrogen exchange precluded the observation of several amino terminal residues. This apparent discrepancy can be explained by the sensitivity of the two techniques to different forms of the protein. Hydrogen exchange selectively observes forms of the protein that are fully or partially unfolded, even when they have extremely low populations, whereas the relaxation measurements are dominated by the most highly populated form of the protein. Thus, these complementary methods indicate that the amino terminal and solvation helices undergo highly restricted fluctuations on short time scales in the folded state but are subject to occasional excursions to an unfolded form with a higher probability than those of the other helices in the TPR repeats.

Concluding Remarks. The dynamics data reported here for two designed TPR proteins confirm that these proteins consist of tandem repeats that are packed fairly rigidly against each other rather than undergoing substantial segmental repeat motions. The local motions of NH groups within each repeat

have the properties that would be expected for well-folded, globular proteins. The dynamics data complement the previous X-ray structures, thermodynamic and kinetic folding data, and hydrogen exchange data. Together, these methods indicate that designed proteins consisting of two or three consensus TPR repeats have very similar physical properties to natural, stable, globular proteins. Thus, the consensus TPR sequence contains sufficient information to specify the interactions both within a single repeat and between adjacent repeats.

ACKNOWLEDGMENT

We thank Joana Tala for the preparation of protein samples, John Tomaszewski and Douglas Brown for helpful discussions, and Lewis Kay (University of Toronto) and Mark Rance (University of Cincinnati) for providing pulse programs.

SUPPORTING INFORMATION AVAILABLE

Tables listing the relaxation and model-free dynamics data for CTPR2 and CTPR3 and assigned HSQC spectra for CTPR2 and CTPR3. This material is available free of charge via the Internet at http://pubs.acs.org.

REFERENCES

1. Main, E. R. G., Jackson, S. E., and Regan, L. (2003) The folding and design of repeat proteins: reaching a consensus, *Curr. Opin. Struct. Biol. 13*, 482−489.
2. Groves, M. R., and Barford, D. (1999) Topological characteristics of helical repeat proteins, *Curr. Opin. Struct. Biol. 9*, 383−389.
3. Main, E. R. G., Xiong, Y., Cocco, M. J., D'Andrea, L., and Regan, L. (2003) Design of stable alpha-helical arrays from an idealized TPR motif, *Structure 11*, 497−508.
4. Zweifel, M. E., Leahy, D. J., Hughson, F. M., and Barrick, D. (2003) Structure and stability of the ankyrin domain of the Drosophila Notch receptor, *Protein Sci. 12*, 2622−2632.
5. Main, E. R., Stott, K., Jackson, S. E., and Regan, L. (2005) Local and long-range stability in tandemly arrayed tetratricopeptide repeats, *Proc. Natl. Acad. Sci. U.S.A. 102*, 5721−5726.
6. Kajander, T., Cortajarena, A. L., Main, E. R., Mochrie, S. G., and Regan, L. (2005) A new folding paradigm for repeat proteins, *J. Am. Chem. Soc. 127*, 10188−10190.
7. Zweifel, M. E., and Barrick, D. (2001) Studies of the ankyrin repeats of the Drosophila melanogaster Notch receptor. 2. Solution stability and cooperativity of unfolding, *Biochemistry 40*, 14357−14367.
8. Bradley, C. M., and Barrick, D. (2002) Limits of cooperativity in a structurally modular protein: Response of the notch ankyrin domain to analogous alanine substitutions in each repeat, *J. Mol. Biol. 324*, 373−386.
9. Ferreiro, D. U., Cho, S. S., Komives, E. A., and Wolynes, P. G. (2005) The energy landscape of modular repeat proteins: Topology determines folding mechanism in the ankyrin family, *J. Mol. Biol. 354*, 679−692.
10. Mello, C. C., and Barrick, D. (2004) An experimentally determined protein folding energy landscape, *Proc. Natl. Acad. Sci. U.S.A. 101*, 14102−14107.
11. Renner, C., Baumgartner, R., Noegel, A. A., and Holak, T. A. (1998) Backbone dynamics of the CDK inhibitor p19(INK4d) studied by 15N NMR relaxation experiments at two field strengths, *J. Mol. Biol. 283*, 221−229.
12. Croy, C. H., Bergqvist, S., Huxford, T., Ghosh, G., and Komives, E. A. (2004) Biophysical characterization of the free I kappa B alpha ankyrin repeat domain in solution, *Protein Sci. 13*, 1767−1777.
13. D'Andrea, L. D., and Regan, L. (2003) TPR proteins: the versatile helix, *Trends Biochem. Sci. 28*, 655−662.
14. Das, A. K., Cohen, P. W., and Barford, D. (1998) The structure of the tetratricopeptide repeats of protein phosphatase 5: implications for TPR-mediated protein-protein interactions, *EMBO J. 17*, 1192−1199.
15. Bruschweiler, R., Liao, X. B., and Wright, P. E. (1995) Long-range motional restrictions in a multidomain zinc-finger protein from anisotropic tumbling, *Science 268*, 886−889.
16. Barbato, G., Ikura, M., Kay, L. E., Pastor, R. W., and Bax, A. (1992) Backbone dynamics of calmodulin studied by 15N relaxation using inverse detected two-dimensional NMR spectroscopy: the central helix is flexible, *Biochemistry 31*, 5269−5278.
17. Tjandra, N., Kuboniwa, H., Ren, H., and Bax, A. (1995) Rotational dynamics of calcium-free calmodulin studied by 15N-NMR relaxation measurements, *Eur. J. Biochem. 230*, 1014−1024.
18. Farrow, N. A., Muhandiram, R., Singer, A. U., Pascal, S. M., Kay, C. M., Gish, G., Shoelson, S. E., Pawson, T., Forman-Kay, J. D., and Kay, L. E. (1994) Backbone dynamics of a free and phosphopeptide-complexed Src homology 2 domain studied by ^{15}N NMR relaxation, *Biochemistry 33*, 5984−6003.
19. Kroenke, C. D., Loria, J. P., Lee, L. K., Rance, M., and Palmer, A. G. (1998) Longitudinal and transverse ^{1}H-^{15}N dipolar ^{15}N chemical shift anisotropy relaxation interference: Unambiguous determination of rotational diffusion tensors and chemical exchange effects in biological macromolecules, *J. Am. Chem. Soc. 120*, 7905−7915.
20. Seewald, M. J., Pichumani, K., Stowell, C., Tibbals, B. V., Regan, L., and Stone, M. J. (2000) The role of backbone conformational heat capacity in protein stability: temperature dependent dynamics of the B1 domain of *Streptococcal* protein G, *Protein Sci. 9*, 1177−1193.
21. Lipari, G., and Szabo, A. (1982) Model-free approach to the interpretation of nuclear magnetic resonance relaxation in macromolecules 1. Theory and range of validity, *J. Am. Chem. Soc. 104*, 4546−4559.
22. Lipari, G., and Szabo, A. (1982) Model-free approach to the interpretation of nuclear magnetic resonance relaxation in macromolecules 2. Analysis of experimental results, *J. Am. Chem. Soc. 104*, 4559−4570.
23. Clore, G. M., Driscoll, P. C., Wingfield, P. T., and Gronenborn, A. M. (1990) Analysis of the backbone dynamics of interleukin-1 beta using two-dimensional inverse detected heteronuclear 15N-1H NMR spectroscopy, *Biochemistry 29*, 7387−7401.
24. Clore, G. M., Szabo, A., Bax, A., Kay, L. E., Driscoll, P. C., and Gronenborn, A. M. (1990) Deviations from the simple 2-parameter model-free approach to the interpretation of ^{15}N nuclear magnetic-relaxation of proteins, *J. Am. Chem. Soc. 112*, 4989−4991.
25. Mandel, A. M., Akke, M., and Palmer, A. G., III (1995) Backbone dynamics of *Escherichia coli* ribonuclease HI: correlations with structure and function in an active enzyme, *J. Mol. Biol. 246*, 144−163.
26. Fushman, D., Xu, R., and Cowburn, D. (1999) Direct determination of changes of interdomain orientation on ligation: Use of the orientational dependence of N-15 NMR relaxation in Abl SH-(32), *Biochemistry 38*, 10225−10230.
27. Smallridge, R. S., Whiteman, P., Werner, J. M., Campbell, I. D., Handford, P. A., and Downing, A. K. (2003) Solution structure and dynamics of a calcium binding epidermal growth factor-like domain pair from the neonatal region of human fibrillin-1, *J. Biol. Chem. 278*, 12199−12206.
28. Hansen, A. P., Petros, A. M., Meadows, R. P., and Fesik, S. W. (1994) Backbone dynamics of a two-domain protein: 15N relaxation studies of the amino-terminal fragment of urokinase-type plasminogen activator, *Biochemistry 33*, 15418−15424.
29. Lee, A. L., Kinnear, S. A., and Wand, A. J. (2000) Redistribution and loss of side chain entropy upon formation of a calmodulin-peptide complex, *Nat. Struct. Biol. 7*, 72−77.
30. Lee, A. L., Sharp, K. A., Kranz, J. K., Song, X. J., and Wand, A. J. (2002) Temperature dependence of the internal dynamics of a calmodulin-peptide complex, *Biochemistry 41*, 13814−13825.
31. Counterman Burba, A. E., Lehnert, U., Yu, E. Z., and Gerstein, M. J-Helix Interaction Tool (HIT): A web-based tool for analysis of helix-helix interactions in proteins, *Bioinformatics*, in press.
32. Munoz, V., and Serrano, L. (1997) Development of the multiple sequence approximation within the AGADIR model of alpha-helix formation: comparison with Zimm-Bragg and Lifson-Roig formalisms, *Biopolymers 41*, 495−509.
33. Walsh, S. T. R., Lee, A. L., DeGrado, W. F., and Wand, A. J. (2001) Dynamics of a de novo designed three-helix bundle protein

studied by N-15, C-13, and H-2 NMR relaxation methods, *Biochemistry 40*, 9560−9569.
34. Cortajarena, A. L., and Regan, L. (2006) Ligand binding by TPR domains, *Protein Sci. 15*, 1193−1198.
35. Jinek, M., Rehwinkel, J., Lazarus, B. D., Izaurralde, E., Hanover, J. A., and Conti, E. (2004) The superhelical TPR-repeat domain of O-linked GlcNAc transferase exhibits structural similarities to importin alpha, *Nat. Struct. Mol. Biol. 11*, 1001−1007.
36. Cliff, M. J., Williams, M. A., Brooke-Smith, J., Barford, D., and Ladbury, J. E. (2005) Molecular recognition via coupled folding and binding in a TPR domain, *J. Mol. Biol. 346*, 717−732.
37. Scheufler, C., Brinker, A., Bourenkov, G., Pegoraro, S., Moroder, L., Bartunik, H., Hartl, F. U., and Moarefi, I. (2000) Structure of TPR domain-peptide complexes: critical elements in the assembly of the Hsp70-Hsp90 multichaperone machine, *Cell 101*, 199−210.
38. Pai, M. T., Yang, C. S., Tzeng, S. R., Wang, C., and Cheng, J. W. (2003) 1H, 15N and 13C resonance assignments of the tetratricopeptide repeat (TPR) domain of hSGT, *J. Biomol. NMR 26*, 381−382.
39. Cliff, M. J., Harris, R., Barford, D., Ladbury, J. E., and Williams, M. A. (2006) Conformational diversity in the TPR domain-mediated interaction of protein phosphatase 5 with Hsp90, *Structure 14*, 415−426.

BI060819A